SOLAR SAIL CAPTURE TRAJECTORIES AT MERCURY

AIAA/AAS Astrodynamics Specialist Conference and Exhibit
5-8 August 2002, Monterey, California

AIAA 2002-4990

Malcolm Macdonald* and **Colin M^cInnes#**

Department of Aerospace Engineering – University of Glasgow,
Glasgow G12 8QQ, Scotland.

ABSTRACT

Mercury is an ideal environment for future planetary exploration by solar sail since it has proved difficult to reach with conventional propulsion and hence remains largely unexplored. In addition, its proximity to the Sun provides a solar sail acceleration of order ten times the sail characteristic acceleration at 1 AU. Conventional capture techniques are shown to be unsuitable for solar sails and a new method is presented. It is shown that capture is bound by upper and lower limits on the orbital elements of the approach orbit and that failure to be within limits results in a catastrophic collision with the planet. These limits are presented for a range of capture inclinations and sail characteristic accelerations. It is found that sail hyperbolic excess velocity is a critical parameter during capture at Mercury, with only a narrow allowed band in order to avoid collision with the planet. The new capture method is demonstrated for a Mercury sample return mission.

INTRODUCTION

Of all the solar planets, Mercury is the least studied, with the exception of Pluto. Only the Mariner 10 spacecraft has ever flown past Mercury, imaging approximately 45% of the surface in 1974-1975 and raising more questions than it answered. Much of what is currently known about Mercury comes from the three Mariner 10 flybys.[1] Earth observations are limited by the proximity of Mercury to the Sun, thus limiting observations to a few hours around dawn and dusk. Important ground-based discoveries include Na, K, and Ca components of the tenuous atmosphere [2,3,4] and radar-reflective polar deposits. [5,6]

A step change in our knowledge of Mercury is required in order to understand how the terrestrial planets formed and evolved. However, direct insertion of a spacecraft into low-Mercury orbit requires a ΔV of approximately 13 km s^{-1}. It was thus considered that insertion of a spacecraft into an orbit about Mercury could not be achieved with conventional propulsion. However, in 1985 it was discovered that with the use of complex sets of gravity assist manoeuvres, it became possible using conventional propulsion to insert a spacecraft into orbit about Mercury. [7, 8] With the recognition of the need to explore Mercury both Europe, with BepiColombo,[9, 10] and the USA, with MESSENGER, plan to utilise gravity assists to place spacecraft into orbit about the planet.

Recent studies have shown that solar sail propulsion can offer a distinct advantage over conventional propulsion systems for Mercury missions. It has been shown that the BepiColombo launch mass can be reduced by over 60% by simply replacing the solar electric propulsion system with a solar sail. [11] Further, it has been shown that a Mercury sample return mission is possible using only a single Soyuz-ST launch, through the utilisation of solar sail technology. [12]

Mercury's close proximity to the Sun results in large propellant mass fractions for conventional propulsion, however such a close perihelion, of only 0.31 astronomical units (AU), results in sail accelerations over ten times the characteristic acceleration at 1AU. This increased acceleration represents a significant manoeuvring capability once captured into orbit at Mercury, either for surface imaging[13, 14] or to manoeuvre the solar sail into a low parking orbit to minimise propellant mass requirements for the descent and ascent stages of a sample return. Since the solar sail does not require propellant mass, launch mass and payload mass fractions are significantly improved relative to chemical and electric propulsion for both orbiter and sample return missions.

CONVENTIONAL CAPTURE TRAJECTORIES

Capture spirals using conventional propulsion (chemical or electric) require the definition of a sphere of influence[15] and the hyperbolic excess velocity of the spacecraft on crossing the sphere of influence. For example, an internal ESA study in 1997 defined Mercury's sphere of influence as 50000 km from the planet centre and hyperbolic excess velocity as 663 m s^{-1} for an electric propulsion transfer, with gravity assists.[16]

A key advantage of solar sailing for interplanetary missions is the ability to depart (and arrive) at a

---

* PhD Research Student, Space Systems Engineering Research Group.
# Professor, Space Systems Engineering Research Group.

planet with zero hyperbolic excess velocity, thus reducing launch mass and cost. While much work has been done on planetary escape using solar sail propulsion,[17] little work has been done on practical capture trajectories. Optimal solar sail interplanetary trajectories define the terminal conditions such that the sail rendezvous' with the target body with zero hyperbolic excess, thus differing from conventional propulsion.

The little work that has been done on solar sail capture trajectories[14, 18] has attempted to comply with the methods employed for conventional propulsion. To generate the quickest possible capture spiral an optimal energy control law is used, with the target orbit about the body defined as the initial orbit and the equations of motion integrated over a negative time span, thus creating a reversed escape spiral which the sail would follow during capture. However, the optimal energy control law can also be called a semi-major axis control law as it can be derived from the variational equation of the semi-major axis,[19] thus such a control law can only control the orbit size and not its shape or orientation. The reversed escape trajectory is propagated to the boundary of the sphere of influence at which point the departure hyperbolic excess velocity, which becomes the arrival velocity, can be found.

This approach has several difficulties. Primarily, convergence with the target orbit is only possible if the sail enters the sphere of influence in exactly the correct manner. That is, the state vectors describing position and velocity at the crossing of the sphere of influence must be matched exactly; otherwise, the shape and orientation of the orbit will not converge with the target orbit, though the size may. Matching the state vectors as the sail crosses the sphere of influence can be very difficult, especially for capture into high inclination orbits. For example, a reversed escape spiral into a similar orbit as described in Ref. 13 and 14, with an arrival date at Mercury of 12 June 2010, requires the sail to have zero hyperbolic excess velocity at a distance of only 15290 km from the centre of Mercury. However, if we delay the arrival at Mercury by six days, until 18 June 2010 corresponding to a delay of less than two thirds of one percent of the interplanetary trip time, we must have zero hyperbolic excess velocity at a distance of 156610 km, an order of magnitude further away. Therefore, if we defined the sphere of influence of Mercury to match the internal ESA study of 1997, Ref. 16, as 50000 km we would require the sail to arrive with either a substantial excess velocity, or to have zero excess velocity at three times the defined sphere of influence, for only a small variation in trip time. Hence, it would be extremely difficult to generate an interplanetary transfer that arrived at Mercury with the correct velocity and position, due to the rapid variation in the position required at the start of any capture spiral using only the semi-major axis control law.

A further difficulty of the reversed escape approach is the inability of the semi-major axis control law to automatically adjust to perturbations not included in the original model. This is analogous to the above scenario, where the sail control law is only able to control the size of the orbit and not its shape and orientation. Additionally, the use of only the semi-major axis control law is prohibitive to very low target orbits about Mercury, as once again, the orbit shape is uncontrolled and hence the trajectory may intersect the planet.

Solar Sail Capture Trajectories

Due to the short orbit periods in low-planetary orbits and consequently rapid variation of the sail control angles, it is computationally intensive to generate optimal solar sail trajectories in a planetocentric environment. Thus, it is not realistic to implement an optimal control system for autonomous on-board sail steering in a planetocentric orbit. However, it has been shown that near-optimal methods can be used to generate the sail control angles in real-time while adjusting for unanticipated orbit perturbations and would thus be suitable as an on-board control scheme.[19, 20] In order to transfer between the optimal interplanetary and near-optimal planetocentric control systems we must define an end and hence corresponding start point for each system.

The prime difficulty identified with the reverse escape approach to Mercury capture was the rapidly varying orientation and velocity at which we require the sail to intersect the planetary sphere of influence. Thus, in identifying a practical capture technique we require the point at which the optimal interplanetary phase terminates to be easily defined and constant throughout the Mercury year, thus enabling the interplanetary trajectory be generated.

In Figure 1, we see the capture orientation illustrated, as the sail passes through the plane perpendicular to the ecliptic and in which both the Sun and Mercury exist. At this point the sail has zero hyperbolic excess velocity and is effectively on a parabolic orbit. The

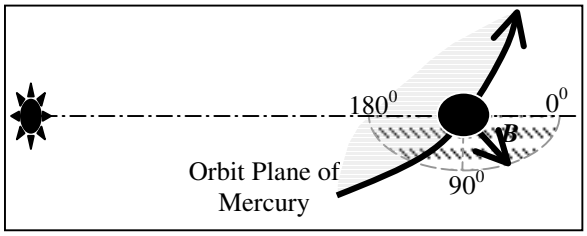

Figure 1 Capture plane shown by dashed region with inclination angle measured within this plane. B-plane aim point is also illustrated within the capture plane.

capture inclination is defined, as shown in Figure 1, to be within the plane of capture and increases from the anti-solar direction in a clockwise sense. Additional to the capture orientation we define a B-plane aim point at which to intercept the planet. Defined as the distance from the planetary surface at which the sail intersects the capture plane and begins its first orbit of the planet, while commencing use of the near-optimal control law.

The near-optimal sail control law is not utilised until the sail passes through the capture plane, as it remains possible to use optimal control theory while considering the effect of Mercury's gravity as a point mass from the edge of the sphere of influence until intersection of the capture plane. Additionally, the effects of planetary oblateness in this short period can be neglected due to the ability of the near-optimal control system to correct for small errors and since Mercury's reciprocal of flattening is almost infinity, making J_2 terms negligible for most Mercury orbits. This short phase could be considered within the interplanetary optimisation problem or perhaps more appropriately as a separate optimisation problem, similar to the method recently proposed for electric propulsion, where the interplanetary trajectory is patched to an inward spiral curve fit through the use of optimal control, solved as a non-linear programming problem using sequential quadratic programming.[21]

In order to achieve a minimum energy Mercury orbit as rapidly as possible we wish to minimise the B-Plane aim point. To find the lowest possible B-plane aim point allowed, while ensuring the solar sail trajectory did not intersect Mercury on completion of the first orbit an investigation was conducted to find the safe bounds which the solar sail must be within. The analysis used a set of modified equinoctial elements, thus avoiding the problems that would occur trying to define and then propagate the initial conditions in classical orbital elements.

Additionally, the different capture inclinations allow the sail to target different orbit inclinations about Mercury, though it has been found that the capture inclination does not always correlate to the final target inclination due to the highly non-linear nature of the equations of motion.[12, 20]

B-PLANE AIM POINT LIMITS

Due to Mercury's highly eccentric orbit, $e = 0.2056$, the solar radiation flux and hence solar sail acceleration significantly vary over the orbit period of Mercury. As a result, the solar sail acceleration varies from approximately 4.5 times greater than the characteristic acceleration value at 1AU, during Mercury aphelion passage, up to over 10.5 times at Mercury perihelion. It thus follows that any given set of safe bounds will vary throughout the Hermian year. However, the arrival date of any sail at Mercury is defined by the duration of the interplanetary cruise phase and is thus not constrained. This is a direct result of the launch date of a solar sail mission not being confined to a launch window. Due to the open nature of the arrival date of a solar sail at Mercury, we are required to define all system boundaries for the worst-case scenario.

In Figure 2 we see the B-plane aim point limits for a range of sail characteristic accelerations, at 1AU, up to 1 mm s^{-2}. Positions above the maximum limit and below the minimum limit will result in the sail colliding with Mercury on completion of the first orbit. The limits are given for a sail passing through the capture plane at zero inclination, i.e. within the orbit plane of Mercury, using the semi-major axis control law and hence insuring the maximum rate of energy loss. It is seen in Figure 2, that the B-plane bounds constrict as the sail acceleration increases, this is shown by both the increase in characteristic acceleration and the variation in the bounds due to the distance of Mercury from the Sun, specifically the bounds are much more constricted at Mercury perihelion than aphelion. We see in Figure 2 the difference between aphelion and perihelion is much more pronounced over the maximum B-plane aim point boundary, where the aphelion case can be as much as 20000 km greater. However, for the minimum B-Plane aim point we see the aphelion boundary is never more than 2500 km from the perihelion case. Finally, from Figure 2 we can note the only effect of orbit perturbations (such as solar gravity, imperfect reflection and Mercury J_2) on the boundaries is to reduce both the upper and lower by approximately 3000 km. However, at low sail accelerations this relationship breaks down, with the lower limit no longer decreasing as sail accelerations drops, due to the increasing importance of the other orbit perturbations as the magnitude of the light perturbation drops toward similar values.

Considering Figure 2, we define the worst or design-case limits when sail arrival coincides with Mercury perihelion passage. We note however, that the greater of the lower limits on B-Plane aim point is at aphelion, but the difference is minimal and since the perihelion maximum is substantially less than the aphelion it was decided to use only the perihelion bounds. Additionally, the extra computational time required (up to 50%) to include orbit perturbations was considered not to merit their inclusion, due to the difference in results shown by Figure 2. Thus, it should be noted that all limits presented are only a guide and not the final definitive answer, which due to Mercury's eccentric orbit and the correspondingly high variations in sail acceleration is extremely difficult to generate.

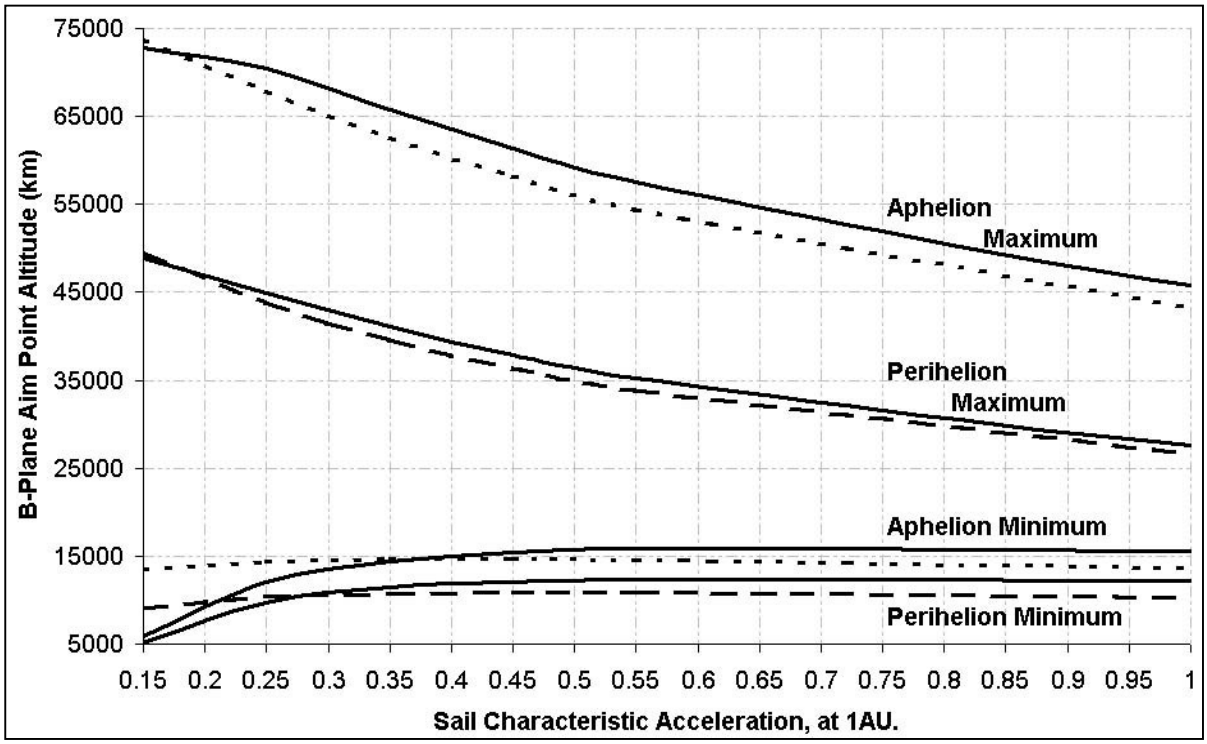

Figure 2 B-Plane Aim point upper and lower bounds for 0^0 capture at Mercury Perihelion and Aphelion, given against sail characteristic acceleration at 1AU. Solid lines correspond to zero perturbation results; dashed lines correspond to model with perturbations included.

It has been noted that optimal Earth – Mercury transfers tend to have clustered arrival dates around Mercury aphelion. With Mercury travelling at its slowest here the effective ΔV is minimised.[22] Therefore, any solar sail arriving at Mercury is unlikely to encounter the worst-case scenario.

B-PLANE AIM POINT LIMITS FOR ALL INCLINATIONS AT MERCURY PERIHELION

Expanding the analysis of B-plane aim point limits beyond the restricted case of capture within the ecliptic plane we can find the upper and lower limits for all capture inclinations. Figure 3 shows the B-plane aim point bounds for a range of near to mid-term sail characteristic accelerations, over the full range of capture inclinations. We again note for capture within the orbit plane of Mercury that the allowed space constricts as we increase the sail acceleration, as was shown in Figure 2.

As the capture inclination is increased, the minimum B-plane aim point decreases. However, as we increase the sail acceleration we see the minimum aim point extend to a higher capture inclination.

For prograde capture inclinations, the maximum B-plane aim point decreases as sail acceleration and/or inclination increase. However, we note for a sail of characteristic acceleration 0.15 mm s^{-2} when capture inclination reaches 75^0 the maximum B-plane aim point passes through a turning point at 35000 km, and very rapidly increases. This turning point is repeated for a sail characteristic acceleration of 0.25 mm s^{-2} when capture inclination reaches 88^0, at 12000 km. However, for higher acceleration sails the turning point happens at negative B-Plane aim points, thus effectively creating a closed zone within which we can safely capture. Additionally, we see for these higher sail accelerations that the maximum aim point curves back on itself. For example, a solar sail with a characteristic acceleration of 0.55 mm s^{-2} can safely capture at an inclination of 86^0 with an aim point of 13000 km, yet the maximum aim point boundary crosses the zero altitude aim point when capture inclination is 84^0. For sail accelerations where the turning point exists below the surface of Mercury, there is an inclination range where it is not possible to safely capture, for a characteristic acceleration of 0.45mms^{-2}, this range is from $84^0 – 89^0$.

For retrograde capture inclinations we see in Figure 3 there is no minimum aim point, however the maximum B-plane aim point is defined when the sail enters a near-rectilinear orbit. As the sail acceleration is increased and/or capture inclination decreased the maximum B-plane aim point for retrograde orbits rapidly decreases, however again we see a sharp turning point in the maximum limit as we approach near-polar capture inclinations. We see in Figure 3 that the maximum retrograde limit for a sail of characteristic acceleration 0.15 mm s^{-2} has a minimum turning point at 112^0 and 14500 km, the limit then increases until it intersects the prograde

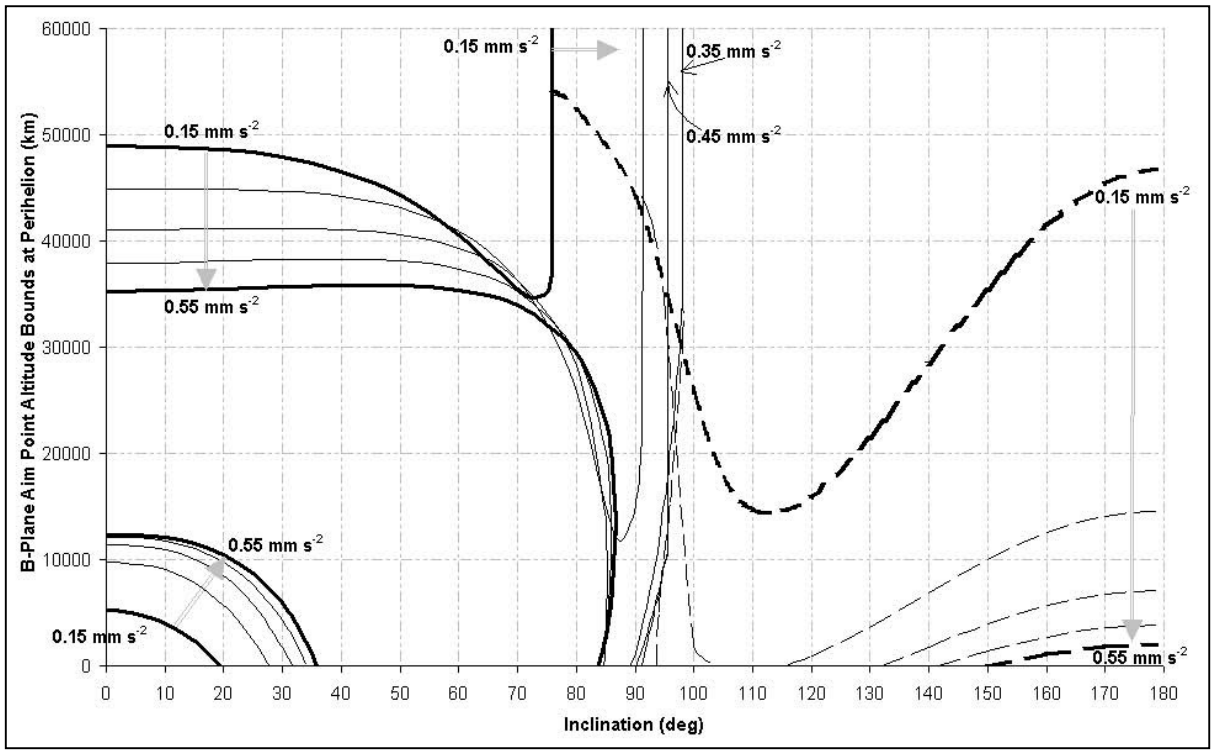

Figure 3 B-Plane aim point upper & lower limits for sail characteristic accelerations between 0.15 mm s^{-2} and 0.55 mm s^{-2}, in increments of 0.1 mm s^{-2} as indicated. The solid lines at the bottom left are minima and the solid lines at the top left are maxima, outside of which results in a collision with Mercury on completion of the first orbit. The dashed lines corresponding to retrograde capture inclinations are maxima, above which the sail will enter a rectilinear orbit.

boundary, as it is rapidly increasing, at 76^0 and 54200 km. We see similar trends for retrograde capture in the upper bounds of all sail accelerations, however as sail acceleration increases once again the turning point occurs at negative B-plane aim points. The rapid increase associated with prograde capture occurs at greater inclinations as sail acceleration is increased, thus the intersection with the retrograde limit occurs at a much lower B-plane aim point. As a result we see in Figure 3 that the region of safe capture at near-polar orbits is very small for high sail accelerations, additionally we note for high sail accelerations it is highly likely a sail will enter a near-rectilinear orbit for most retrograde capture inclinations. For a characteristic acceleration of 0.55mm s^{-2} it is found that safe capture cannot be performed for inclinations between 85^0 and 150^0, meaning after capture a period of orbit cranking would be required to achieve a polar orbit.

HYPERBOLIC EXCESS VELOCITY LIMITS

All propulsion systems have a maximum hyperbolic excess velocity, above which it is not possible to capture into a closed orbit about a target body. For conventional chemical propulsion, the maximum excess velocity is defined by the propellant mass budget on-board. However, for a solar sail the maximum excess velocity is defined by the sail characteristic acceleration. An investigation was conducted to find out what levels of excess velocity could safely be carried through the capture plane, for the restricted case of capture within the ecliptic plane.

It was found that a minimum hyperbolic excess velocity limit could be defined for B-plane aim points below the defined minimum aim point of any given sail acceleration. Thus, we can now say there is no minimum B-plane aim point, instead there is a required minimum hyperbolic excess velocity for safe capture below the previously defined minimum aim point. For a fixed aim point the required excess velocity increases as sail acceleration is increased, this is shown in Figure 4.

Figure 4 shows that as the sail acceleration is increased the maximum hyperbolic excess velocity limit increases, as we would expect. However, due to the constriction of allowed space with increased sail acceleration associated with the upper B-plane aim point boundary, as shown by Figures 2 & 3, we see the maximum excess velocity drops off to zero at lower B-plane aim points as sail acceleration is increased.

It should be noted that for hyperbolic excess velocities above the maximum defined in Figure 4 result in the sail colliding with Mercury on completion of the first orbit and not in a planetary fly-

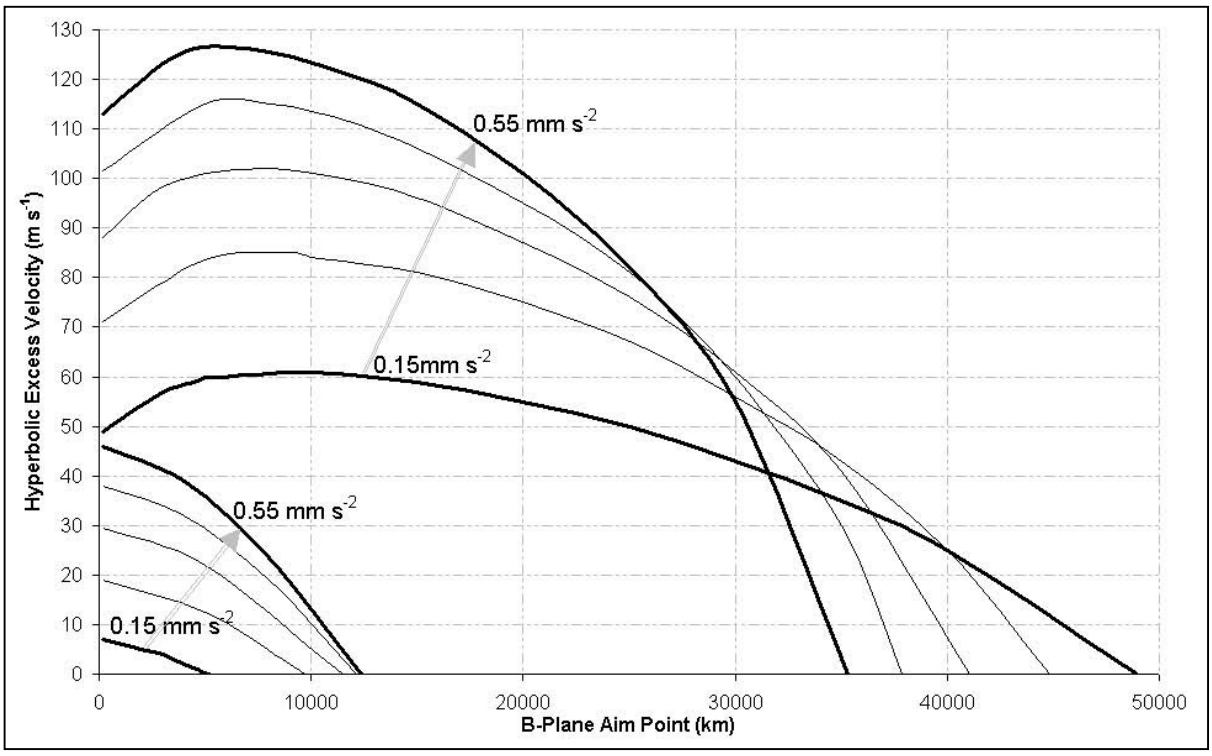

Figure 4 Hyperbolic Excess Velocities for capture at anti-solar intersection of Mercury's orbit plane and the capture plane, ranging from Mercury's surface to the maximum B-Plane aim point. Minimum limits are at the bottom left below which results in collision with Mercury on completion of the first orbit, similarly above the maximum limit also results in collision with mercury on completion of the first orbit.

past as may be expected, the bound for this is much higher due to the optimal energy sail steering law that was used.

Though we see in Figures 2, 3 & 4 the safe region of B-plane aim points constricts as sail acceleration is increased it should be noted that the rate at which the upper and maximum bounds contract is not constant and as such no maximum sail acceleration was detected. Similarly, no minimum exists.

Example of Solar Sail Capture at Mercury

Perhaps the most compelling mission utilising solar sail propulsion at Mercury is the recently proposed sample return mission, Ref. 12, where the mass budget provides for a single Soyuz-ST launch vehicle. Solar sail propulsion is an enabling technology, providing a realistic mission scenario for Mercury sample return missions. A key feature of such missions is the ability of a solar sail to spiral into a very low, 125 km near-polar circular orbit hence significantly decreasing the lander propellant mass requirements. Autonomous solar sail steering would further reduce mission costs, and as already been stated the optimal energy control law tends to generate trajectories that intersect the planet surface when used for very low altitude orbit manoeuvring. Hence, the near-optimal blending of control laws is essential in order to safely achieve low Mercury orbits, with the additional benefit of being suitable as an on-board real-time sail control system. The methods outlined in this paper, and Refs. 19, 20, have been utilised in order to generate capture trajectories that apply to such Mercury sample return missions.

An open launch window from Earth is considered and as such, launch date is arbitrarily set as 1 January 2015, providing an arrival date at Mercury of 25 April 2018.

We use a B-plane aim point of 200 km for arrival at Mercury, with a capture inclination of 68^0, reflecting the complex nature of the safe capture region at near-polar inclinations. The capture spiral is shown in Figure 5.

The near-optimal control law blends individual control laws for each orbit element by a system of weighted averages defined by the orbit elements, hence as an element approaches its target value the weighting applied to its control law reduces. This system differs from the conventional approach to blending control laws, which sets each weight as a function of time, hence reducing system autonomy.

The control law used in Figure 5 blended control laws for semi-major axis, eccentricity, inclination and radius of pericentre, [19] generating a capture spiral to

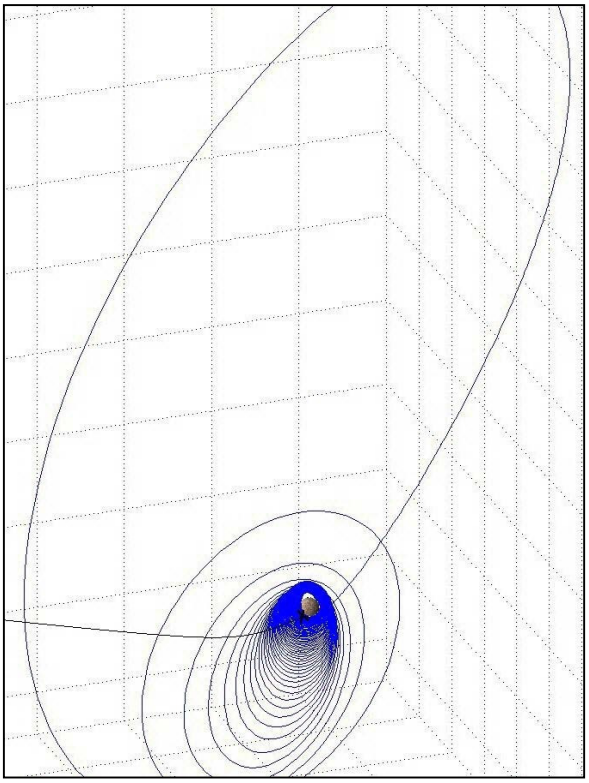

Figure 5 Solar sail capture at Mercury, into a near polar, circular 125 km altitude orbit.

125 km altitude and a final inclination of 88^0. Additionally, arrival at the final orbit is such that it coincides with Mercury aphelion passage, hence reducing thermal loads on the lander and spacecraft.

Conclusions

Conventional capture techniques have been shown to be inappropriate for solar sail propulsion and a new approach has been detailed. A significant advantage of the approach outlined in this paper is the clear definition given to the end of the optimal interplanetary mission phase and the start of the planetocentric phase, where optimal control cannot be used. This patch point does not exist using conventional techniques making the generation of useful interplanetary trajectories much more difficult as the terminal conditions are constantly varying in an unpredictable manner. It should be noted that the variation of the terminal conditions is much larger than for electric propulsion, due to the inability of a solar sail to continuously direct its force vector along the negative velocity vector, causing a much larger variation in orbit eccentricity during the escape spiral.

The upper and lower limits on the position and velocity of a solar sail as it intersects the capture plane have been presented for a range of near to mid-term sail characteristic accelerations. It was shown the safe capture region, for both position and velocity, constricts as sail acceleration is increased, due to Mercury's proximity to the Sun and/or an increase in sail acceleration. However, no maximum sail acceleration was found, as the rate of constriction falls away as acceleration increases. Additionally, we note knowledge of sail velocity is of greater importance as the bounds are much narrower than those for position, though neither should not pose a significant navigation risk.

It was shown that capture into a retrograde inclination is difficult and tends to result in a near-rectilinear orbit. Additionally, it is shown that capture directly into polar orbits is difficult for high sail accelerations.

Finally, the capture technique has been demonstrated for a Mercury sample return type orbit, where the sail captures into a 125 km near-polar circular orbit.

References

[1]Vilas, F., Chapman, C.R., Matthews, M.S. (Eds.), 'Mercury', University of Arizona Press, Tucson, 1998.

[2]Potter, A.E., Morgan, T.H., 'Discovery of sodium in the atmosphere of Mercury', Science, **229**, 1985, pp 651 –653.

[3]Potter, A.E., Morgan, T.H., 'Potassium in the atmosphere of Mercury', Icarus, **67**, 1986, pp336 –340.

[4]Bida, T.A., Killen, R.M., Morgan, T.H., 'Discovery of calcium in Mercury's atmosphere', Nature, **404**, 2000, pp 159 –161.

[5]Slade, M.A., Butler, B.J., Muhleman, D.O., 'Mercury radar imaging: evidence for polar ice', Science, **258**, 1992, pp 635 –640.

[6]Harmon, J.K., Slade, M.A., 'Radar mapping of Mercury: full-disk images and polar anomalies', Science, **258**, 1992, pp 640 –642.

[7]Yen, C.-W., 'Ballistic Mercury orbiter mission via Venus and Mercury gravity assists', AIAA 85-346, AAS/AIAA Astrodynamics Specialist Conference, San Diego, California, 1985.

[8]Yen, C.-W., 'Ballistic Mercury orbiter mission via Venus and Mercury gravity assists' J. Astron. Sci, **37**, 1989, pp 417-432.

[9]'BepiColombo The Interdisciplinary Cornerstone Mission to the Planet Mercury' An Overview of the System and Technology Study, ESA-SCI(2000)2, September 2000.

[10]Anselmi, A., Scoon, G.E.N., 'BepiColombo, ESA's Mercury Cornerstone mission', Planetary and Space Science, **49**, 2001, pp 1409-1420.

[11]M^{c}Innes, C.R., ' Solar Sail Missions and Technology Requirements', Contract No. 13848/99/NL/MV for ESA-ESTEC, November 2000.

[12]M^{c}Innes, C.R., Hughes, G., Macdonald, M., "Low Cost Mercury Orbiter and Sample Return Missions using Solar Sail Propulsion", DR-0113, Nov. 2001.

[13]Leipold, M.E., Wagner, O., 'Mercury Sun-Synchronous Polar Orbits Using Solar Sail Propulsion', J. Guidance, Control and Dynamics, **19**, 1996, No.6, pp 1337-1341.

[14]Leipold, M.E., Sebolt, W., Lingner, S., Borg, E., Herrmann, A., Pabsch, A., Wagner, O., Brückner, J., 'Mercury Sun-Synchronous Polar Orbiter with a Solar Sail', Acta Astronautica, **39**, 1996, No. 1-4, pp. 143-151.

[15]Roy, A.E., 'Orbital Motion', Institute of Physics Publishing, London, 1998 (pbk).

[16] Racca, G.D., 'Mercury Orbiter Mission with Solar Electric Propulsion', Internal Memorandum, ESA/PF/1440.97/GR, April, 1997.

[17]Coverstone-Carroll, V., Prussing, J.E., 'A Technique for Earth Escape Using a Solar Sail' AAS 99-333, AAS/AIAA Astrodynamics Specialist Conference, Westin Prince Alyeska Resort, Girdwood, Alaska, 1999.

[18]Wright, J. L., 'Space Sailing', Lerner Publications Company, Minneapolis, 1994.

[19]Macdonald, M., M^{c}Innes, C.R., 'Analytic Control Laws for Near-Optimal Geocentric Solar Sail Transfers', AAS 01-472, AAS/AIAA Astrodynamics Specialist Conference, Québec City, Québec, 30 July – 2 August 2001.

[20]Macdonald, M., M^{c}Innes, C.R., 'Safe Capture and Escape Control Algorithms for Solar Sails', to be submitted to Journal of Guidance, Control and Dynamics, May-June 2002.

[21] Kluever, C.A., 'Optimal Earth-Capture Trajectories Using Electric Propulsion', J. Guidance, Control and Dynamics, **25**, No. 3, pp 604-606, 2002.

[22]Hughes, G., 'Personal Communiqué', University of Glasgow, Glasgow, Scotland, April 2002.